

CATCHMENT PROPERTIES IN THE KRUGER NATIONAL PARK DERIVED FROM THE NEW TANDEM-X INTERMEDIATE DIGITAL ELEVATION MODEL (IDEM)

J. Baade ^{a,*}, C. Schmullius ^b

^a Department of Geography, Physical Geography, Friedrich-Schiller-University Jena, 07737 Jena, Germany – cub@uni-jena.de

^b Department of Geography, Earth Observation, Friedrich-Schiller-University Jena, 07737 Jena, Germany – c.schmullius@uni-jena.de

KEY WORDS: TanDEM-X, ASTER GDEM2, SRTM, RTK-GNSS, validation, watershed delineation, Savanna, South Africa,

ABSTRACT:

Digital Elevation Models (DEM) represent fundamental data for a wide range of Earth surface process studies. Over the past years the German TanDEM-X mission acquired data for a new, truly global Digital Elevation Model with unpreceded geometric resolution, precision and accuracy. First processed data sets (i. e. IDEM) with a geometric resolution of 0.4 to 3 arcsec have been made available for scientific purposes. This includes four $1^{\circ} \times 1^{\circ}$ tiles covering the Kruger National Park in South Africa. Here we document the results of a local scale IDEM validation exercise utilizing RTK-GNSS-based ground survey points from a dried out reservoir basin and its vicinity characterized by pristine open Savanna vegetation. Selected precursor data sets (SRTM1, SRTM90, ASTER-GDEM2) were included in the analysis and highlight the immense progress in satellite-based Earth surface surveying over the past two decades. Surprisingly, the high precision and accuracy of the IDEM data sets have only little impact on the delineation of watersheds and the calculation of catchment size. But, when it comes to the derivation of topographic catchment properties (e.g. mean slope, etc.) the high resolution of the IDEM04 is of crucial importance, if - from a geomorphologist's view - it was not for the disturbing vegetation.

1. INTRODUCTION

Digital Elevation Models (DEM) represent fundamental data for a range of applications including Earth surface process studies in the field of ecology, geology, geomorphology and hydrology, among others. For some countries high resolution Digital Terrain Models (DTM) representing the solid Earth surface derived from topographic maps or aerial surveys (photogrammetry, laser) are available. But, for vast regions of the Earth this fundamental data is missing. Starting with the Shuttle Radar Topographic Mission (SRTM) in February 2000, the past two decades have witnessed a continuous growth in the use of satellite-based data for the production of DEMs. Being based on either Synthetic Aperture Radar (SAR) interferometry like the suite of SRTM SIR-C products (Farr et al., 2007), or optical images like the ASTER-GDEM (ASTER GDEM Validation Team, 2011) these elevation models represent the surface of the Earth including the height of the land cover (vegetation, buildings and other objects). Thus, these DEMs are often considered Digital Surface Models (DSM) as compared to DTMs.

Since December 2010 the German radar satellite mission TanDEM-X acquired data for a new and truly global Digital Elevation Model (DEM) with unpreceded geometric resolution, precision and accuracy (Krieger et al., 2013; Zink and Moreira, 2014). According to Bräutigam et al. (2014) data acquisition was expected to conclude by August 2014 and the finalization of the global DEM by the end of 2015. Since November 2014 processed data sets from the first year's acquisition (i. e. the Intermediate DEM, IDEM) with a geometric resolution of up to 0.4 arcsec (~12 m)(IDEM04) at the equator are available for selected regions of the World for scientific purposes. This includes four $1^{\circ} \times 1^{\circ}$ tiles covering almost the entire Kruger

National Park (KNP) in South Africa. In addition, IDEM tiles with 1 arcsec (IDEM10, ~30 m) and 3 arcsec (IDEM30, ~90 m) resolution were made available. Due to the fact that the TanDEM-X derived height measurements include land cover, the IDEM data sets have to be considered DSMs.

This paper reports on the application of the three IDEM data sets for the delineation of hydrological catchments and the derivation of catchment properties in a pristine Savanna environment, i.e. the Kruger National Park (KNP) in the Northeast of the Republic of South Africa (RSA). This includes an accuracy assessment utilizing RTK-GNSS-based ground survey points from a dried out reservoir basin and its vicinity. In order to test the connotation of an unpreceded precision and accuracy, the pertinent, global, open access precursor DSMs, i.e. SRTM1, SRTM90 and ASTER-GDEM2, were included in the analysis.

2. MATERIAL AND METHODS

2.1 Study site

The study is conducted in the southern part of Kruger National Park (KNP) located in the northeastern part of the Republic of South Africa (KNP). In total, the KNP occupies about 19,500 km² of the undulating Lowveld Savanna between the foot slopes of the Drakensberg Escarpment to the west and the coastal plains of Mozambique to the east (Figure 1). Its N–S extension is about 350 km and its W–E extension ranges from 35 to 70 km. The landscape pattern within KNP follows in general the NNW–SSE strike of the major geological units characterized by granitic rocks and the basement complex in the west and the Karoo sedimentary and volcanic rocks in the east (Venter et al., 2003). Most parts of what became KNP in 1926

* Corresponding author.

have not been attractive to white farmers because of mosquito and tsetse fly infestation and were set aside for the recovery of wildlife in the first decade of the 20th century (Carruthers, 1995). Thus, most parts of the KNP have never experienced an enhanced European style agricultural development and can be considered to represent a pristine Savanna environment. In particular, this study focusses on the catchment areas of 21 fresh water reservoirs (Figure 1) constructed in the second half of the last century in the framework of a water provisioning programme. At the time of the IDEM data acquisition some of the reservoirs were breached and dried out while others were still intact and contained water.

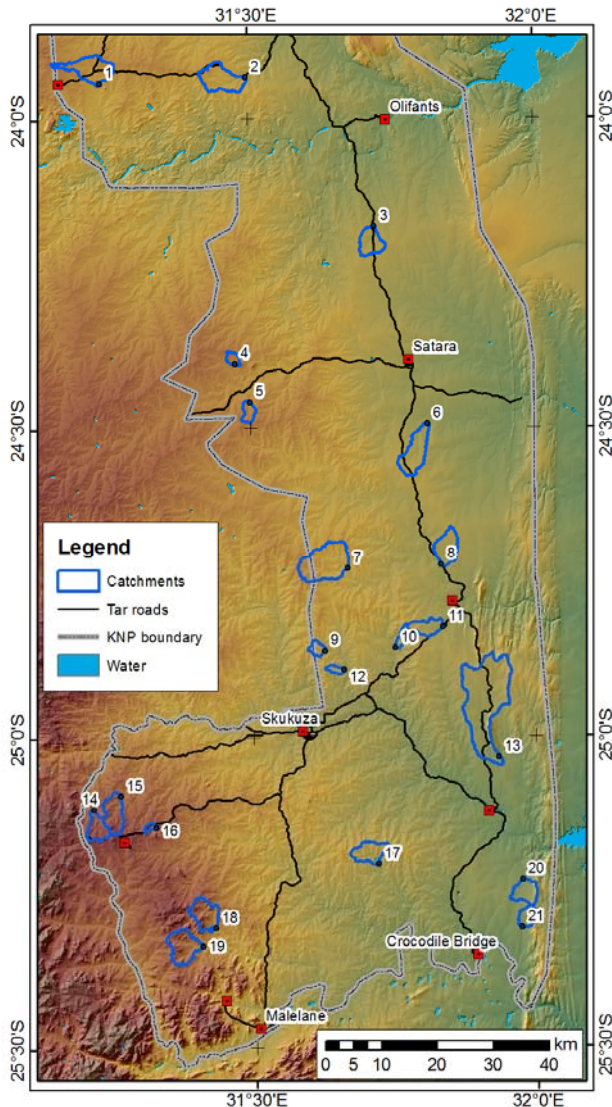


Figure 1. Location of studied catchments within the southern part of Kruger National Park, South Africa
 (IDEM30 source: [©]DLR 2014).

2.2 Properties of the DSM data sets

For this study three high resolution IDEM04, three medium resolution IDEM10 as well as six low resolution IDEM30 tiles as well as the corresponding medium resolution ASTER GDEM2 and SRTM1 and the low resolution SRTM90 data sets (Table 2) were mosaicked. The general properties of the IDEM data sets were analysed for the wider study area, i.e. the

southern part of the Kruger National Park, covering 11,500 km². The general properties of the IDEM data sets are documented in a number of auxiliary files, e. g. layover and shadow mask (LSM), coverage map (COV), height error map (HEM), and a water indication mask (WAM) (Wessel et al., 2013). Due to the rather flat terrain of the Lowveld (Figure 1), layover and shadow is not an issue of concern. Less than 0.01 % of all pixel are affected. The coverage map indicates, that 60 %, 36 % and 4 % of all pixel represent data from one, two and three acquisitions, respectively.

The HEM, representing the uncertainty induced by the interferometric coherence and the geometry, provides values between < 0.01 m and 115 m with a mean value of 0.56±0.25 m for the IDEM04 mosaic covering the southern part of KNP. About 1 % of all pixel exhibit a height error ≥ 1.0 m, but less than 0.01 % have an error ≥ 10.0 m (Figure 3). Analysing the HEM for the IDEM10 and IDEM30 provides very similar mean uncertainties, but higher minimum and lower maximum errors. This provides first evidence for the overall high precision of the TanDEM-X instrument and the data processing chain.

Pixels affected by water are identified in the WAM based on several criteria. However, one need to bear in mind that *islands with an area smaller 1 hectare and water bodies with an area smaller 2 hectare are not considered* (Wessel et al., 2013, p. 18). This threshold does not pose a problem when dealing with compact water bodies like reservoirs and lakes. But it clearly makes it more difficult to identify height pixels affected by water along the course of rivers, often inducing disrupted sinks when pixels affected by water are masked (Figure 1).

	Resolution		
	Geometric (arcsec)	data format	Acquisition
IDEM04	0.4	float	X-SAR
IDEM10	1	float	X-SAR
IDEM30	3	float	X-SAR
ASTER GDEM2	1	integer	Optical
SRTM1	1	integer	SIR-C
SRTM90	3	integer	SIR-C

Table 2. Properties of the DEM data sets used in this study

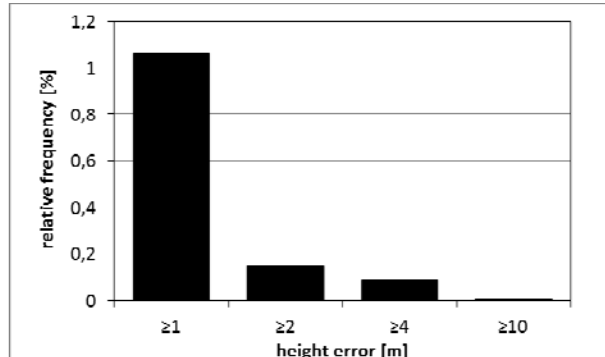


Figure 3. Relative frequency [%] distribution of IDEM04 height error classes (≥ 1 m) within the southern part of KNP. Note: over 98 % of all pixel are associated with a height error < 1 m.

Unfortunately, none of the other DSM data sets include detailed, i.e. pixel specific, quality assessment files. Therefore, a study site specific a priori introduction to the properties of

these data sets is inhibited. Nonetheless, pertinent accuracy assessment reports are available and will be used in the discussion of the results.

2.3 Accuracy assessment using ground measurements

Recently, Wessel et al. (2014) used ICESat validation points, kinematic GPS (KGPS) tracks with an accuracy of < 1 m and SRTM data to assess the accuracy of IDEM04 tiles on the global scale. Here, we utilize Real Time Kinematic (RTK) GNSS based survey points from a dried out reservoir basin (Silolweni, no. 11 in Figure 1) devoid of woody vegetation and its vicinity characterized by open, woody Savanna vegetation (Figure 4) for a local scale assessment of the accuracy of the IDEM data sets. The survey points ($N = 1088$ points) were measured in February and September 2014 using LEICA GS10 and GS15 GNSS receivers equipped with a radio connection. The base station position was determined with reference to the South African network of permanent GNSS stations (TrigNet). The accuracy of the point heights is < 0.05 m for height above ellipsoid (HAE) and ~ 0.10 m for height measures referenced to the geoid (ALT). Thus, the absolute accuracy of the survey points is much better than the precision of the height measures from the IDEM data sets as well as the other DSM data sets.



Figure 4. View of the dried out Silolweni reservoir basin and its vicinity used for IDEM accuracy assessment. The distance to the far end is about 650 m. The bigger trees at the far end reach heights of about 10 m (photo: J. Baade, Sep. 2014).

In order to weight each DSM pixel equally, multiple survey point samples within a DSM pixel were averaged (Rodrigues et al., 2006) taking into account the detailed geometry of the raster data sets to compare with. Thus, the ~ 1100 individual survey points were reduced to 765 pixel with 0.4 arc sec resolution and 370 and 75 pixel with 1 arc sec and 3 arc sec resolution, respectively. The difference between ground survey heights (RTK heights) and DSM heights was calculated by subtracting RTK heights from DSM heights. In accordance with other validation efforts (e.g. ASTER GDEM Validation Team, 2011) this yields positive differences for all DSM pixel characterized by a vegetation cover dense and high enough to bias the height measure in the DSM.

2.4 Watershed delineation and catchment properties

In order to derive a hydrological correct elevation model the IDEM data sets representing heights above the WGS84 ellipsoid (HAE) (Wessel et al., 2013) were transformed to heights above the geoid (ALT) using the most recent hybrid

geoid model for South Africa, the SAGEOID10 (Chandler and Merry, 2010). This geoid model is provided with a 1 arcsec geometric resolution and an accuracy of about 7 cm. The geoid model was accordingly resampled and finally the transformed DSM was projected to UTM36S. No attempts were made to remove or manipulate pixel, especially from the high resolution IDEM04 clearly representing canopy height or single trees. However, all sinks were filled prior to the performance of the hydrological analysis.

The calculation of the flow direction and flow accumulation grids as well as the consecutive batch watershed delineation for the reservoirs was conducted using standard routines implemented in Arc Hydro Tools for ArcGIS 10.2 (Esri Water Resources Team, 2014). Due to the fact that the routing of runoff over the digital elevation model changes with the resolution of the grid, some manual user interaction was needed to adjust the catchment outflow point and ensure a correct delineation of the watersheds.

In addition to catchment area representing the primary catchment property, we report here on the variation of catchment wide slope estimates.

3. RESULTS AND DISCUSSION

3.1 Accuracy assessment based on ground survey points

The RTK-GNSS based bare ground height measurements averaged for the IDEM04 conform 0.4 arc sec pixel ($N = 767$) in the dried out Silolweni reservoir basin and its vicinity range from 282.80 to 294.60 m HAE (Figure 4) over an area of about 0.5 km². Compared to this, the IDEM04 height readings range

	N	Height measure	RMSE
IDEM04	767	HAE	1.55
IDEM10	368	HAE	1.46
IDEM30	76	HAE	1.65
GDEM2	368	ALT	5.9
SRTM1	368	ALT	5.7
SRTM90	72	ALT	5.9

Table 5. Summary statistics of the height difference between pixel based averaged ground survey point measures and DEM pixel values [in m], HAE refers to the WGS84 ellipsoid, ALT refers to the EGM96 geoid.

	Min	Mean	1σ	90 %	Max
RTK - IDEM04	-3.65	0.70	1.40	< 2.51	7.85
IDEM04 (HEM)	0.26	0.4	0.1	< 0.52	1.30
RTK - IDEM10	-2.05	0.83	1.20	< 2.45	7.88
IDEM10 (HEM)	0.29	0.41	0.06	< 0.49	0.75
RTK - IDEM30	-0.78	1.25	1.07	< 2.75	4.28
IDEM30 (HEM)	0.32	0.41	0.04	< 0.46	0.52
RTK - GDEM2	-14.2	1.9	5.6	< 9.60	18.7
RTK - SRTM1	0.6	5.4	1.9	< 7.60	12.3
RTK - SRTM90	1.6	5.6	1.7	< 7.55	10.6

Table 6. Detailed statistics of the height difference between pixel based averaged ground survey point measures and DEM pixel values [in m]

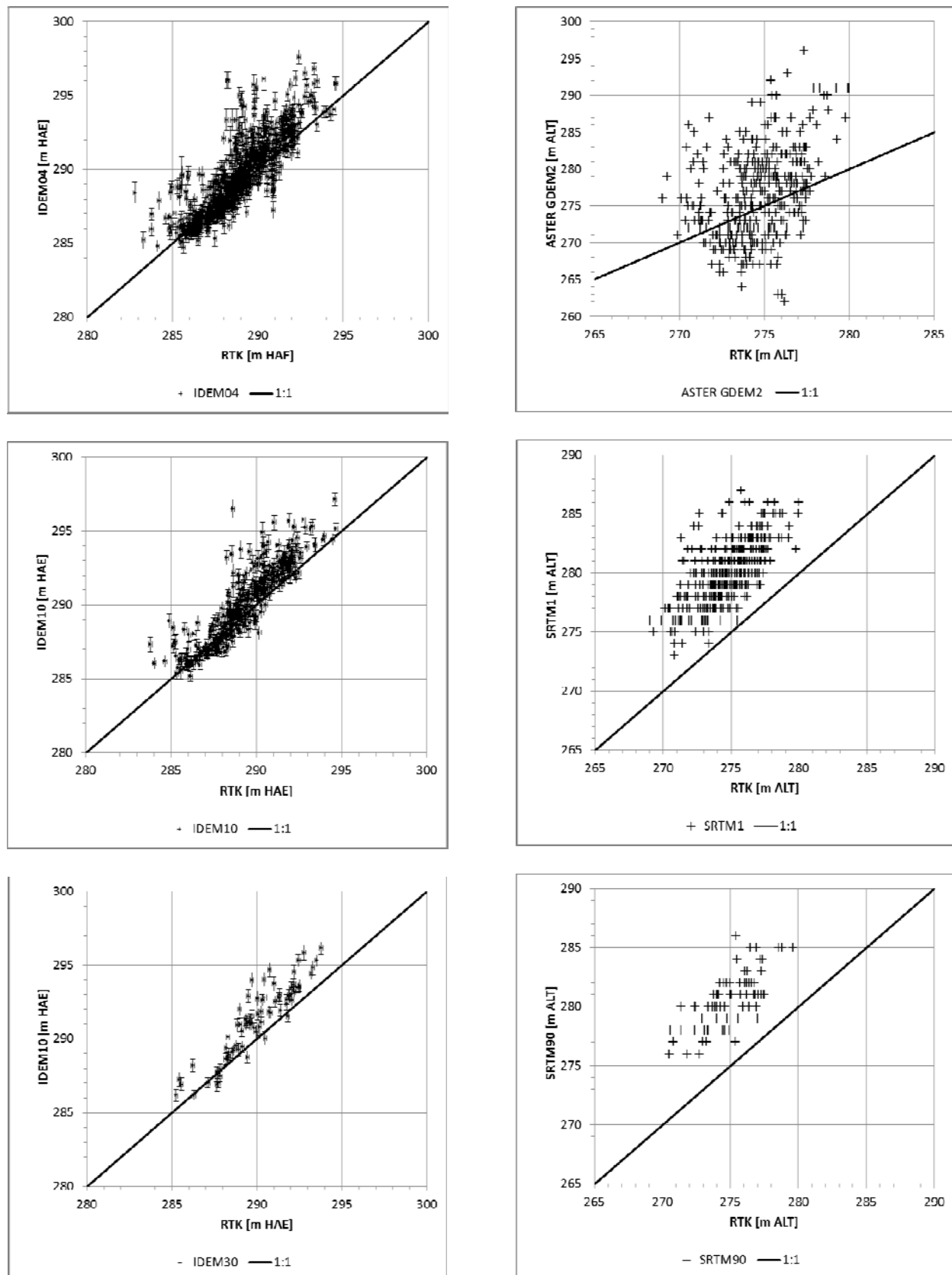


Figure 7. Absolute height difference scatter plots derived from the comparison of RTK-GNSS based ground survey points and DEM pixel heights. For the IDEM data sets the height is given in m HAE and the precision of the measurement is indicated with whiskers.

For the other data sets height is given in m ALT (data sources: IDEM: ©DLR 2014, ASTER GDEM2 is a product of METI and NASA, SRTM1: USGS 2014, SRTM90: Jarvis et al. 2008).

from 284.70 to 297.60 m HAE. The RMSE yields a value of 1.55 m (Table 5). The mean difference is 0.7 m and thus slightly larger than the mean precision of the IDEM04 data (HEM) for all pixel analysed here (0.4 ± 0.1 m) (Table 6). With a maximum height difference of ~ 7.9 m and 90 % of all absolute height errors < 2.5 m, the IDEM04 data set clearly fulfils the accuracy benchmark for the TanDEM-X mission (Krieger et al., 2013). This holds as well for the lower resolution IDEM products showing very similar RMSE values (Table 5) as well as detailed statistical characteristics (Table 6).

Inspection of the absolute height difference scatter plots (Figure 7) provides evidence for the IDEM products of a distribution in accordance with the expectation. There is a clear general trend of increasing IDEM height readings with increasing ground survey point heights. This indicates that the IDEM products represent the changes in relief in this rather flat terrain quite well. Basically, the height differences are distributed symmetrically around the one-to-one line. However, there is an increase of the height difference with increasing ground survey point height. This is in accordance with the landscape characteristics within the dried out Silolweni reservoir basin and its vicinity. The reservoir is virtually bare of woody cover while the elevated surroundings of the reservoir basin are characterized by an open woody Savanna vegetation reaching heights of about 10 m (Figure 3). The high scatter at the lower end of the point cloud can be explained by pixel representing thalwegs leading in and out of the reservoir basin covered by rather dense riparian forests. Thus, positive height differences can be easily explained by the fact that the X-band radar backscatter originates from the vegetation canopy and not the bare ground (Wessel et al., 2013; Baade & Schmullius, 2014).

However, the scatter plot shows as well a considerable number of observations with rather large negative deviations, i.e. well beyond the maximum height error (1.3 m acc. to HEM), especially for the IDEM04 data set. An in depth analysis of these phenomenon is beyond the scope of this paper. But, it seems that these pixels are often associated with surface features like the earthen dam of Silolweni reservoir or gullies orientated perpendicular to the line of sight of the TanDEM-X instrument and being smaller than the resolution cell.

The statistics (Table 5, Table 6) and the scatter plots (Figure 7) for the other three data sets show clearly higher RMSE values as well as much stronger scatter of the height differences. This holds especially for the ASTER GDEM2 data set. Here, the scatter plot basically suggests strong random errors. Fitting a linear model to the point cloud reveals that only 15 % of the variation in ASTER GDEM2 height readings is attributable to changes in bare ground heights and suggests that the ASTER GDEM2 does not represent the changes in relief in this rather flat terrain adequately.

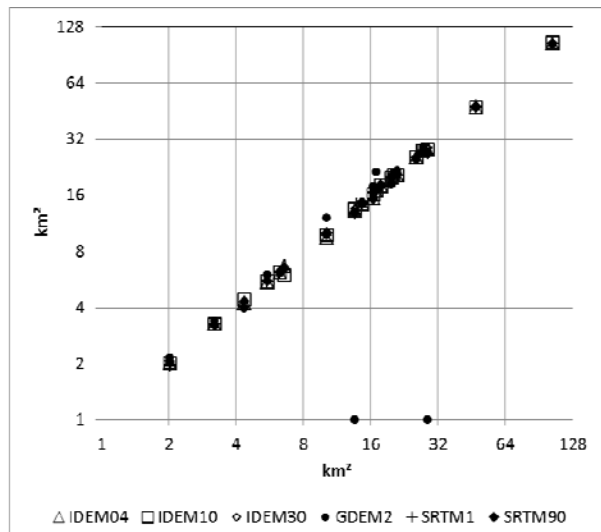
Despite of the higher RMSE values for the SRTM1 and SRTM90 data set, the corresponding scatter plots resemble the IDEM scatter plots in appearance. Both SRTM scatter plots show a general trend of increasing DSM height readings with increasing bare ground height measurements. This, again, indicates that both SRTM products reproduce the changes in relief. In contrast to the IDEM products, height differences for the SRTM products are all positive. The mean height difference is about 5.5 m. About 10 % of the observed height difference might be attributed to the different geoids applied. The SRTM products are referenced to the EGM96 geoid, while we used the SAGEOID10 to transfer RTK-GNSS height measurements from

m HAE to m ALT. Apart from this, the mean height difference corresponds well to the 5.6 m absolute height error identified for the African continent during the SRTM performance analysis (Farr et al., 2007). The fact that the maximum height differences are larger for the SRTM product than the ones observed for the IDEM products is of a surprise. Due to the longer radar wavelength used in the SRTM mission (C-band with 5.66 cm) (Farr et al., 2007) compared to the TanDEM-X mission (X-band with 3.1 cm) (Krieger et al. 2013) one would expect a better penetration of the canopy cover during the SRTM mission. However, the timing of the SRTM mission corresponds to the leaf-on season in this part of South Africa and might have offset the effects of the different wave lengths.

3.2 Watershed delineation and catchment area

The application of the three IDEM products and the other DEMs for the delineation of the watershed using Arc Hydro Tools for ArcGIS 10.2 (Esri Water Resources Team, 2014) was tested using 21 catchments of reservoirs within the KNP (Figure 1) ranging in size from a few km² to about 100 km². Minor manual user interaction was used to adjust the catchment outflow points to the automatically derived thalweg pattern.

With one exception, i.e. the ASTER GDEM2, all analysed DSM provided reasonable and consistent results (Figure 8). The analysis based on the ASTER GDEM2 failed in two cases to provide any catchment area extending beyond the immediate vicinity of the outflow points. This was due to the development of an erroneous thalweg pattern (Figure 9). In addition, the ASTER GDEM2 provided in some other cases rather large deviations from the SAR-based DSM estimations (Figure 8).



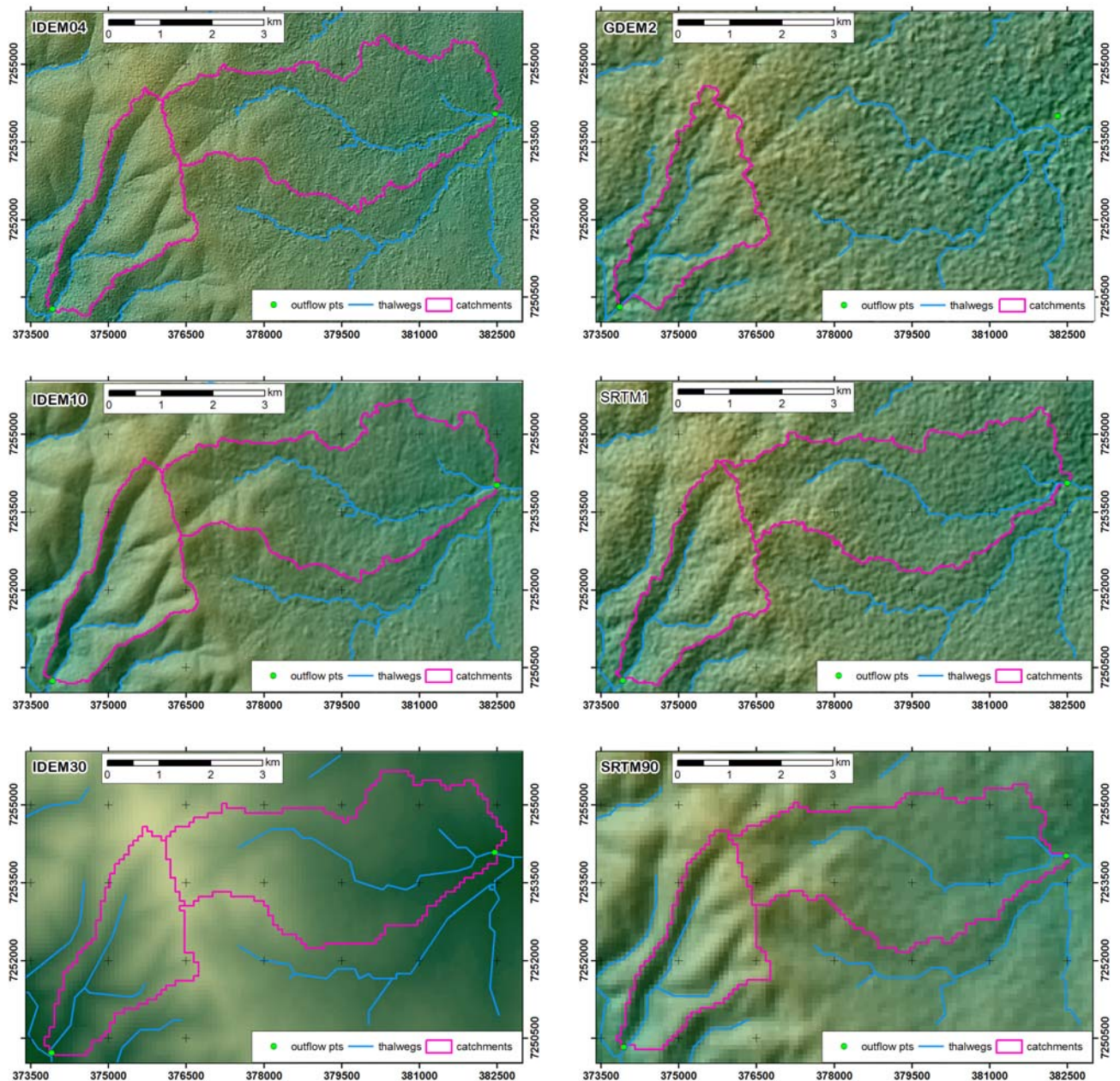


Figure 9. Detailed comparison of DEMs (combined height and hill shade representation) used in this study for runoff routing (thalwegs with 1 km² upstream contributing area) and catchment area delineation. The catchments shown in this figure are the Jones-se catchment (ID No. 10 in Figure 1 and Table 10) to the left and Silolweni (ID No. 11) to the right (data sources: IDEM: [©]DLR 2014, SRTM1: USGS 2014, ASTER GDEM2 is a product of METI and NASA, SRTM90: Jarvis et al. 2008).

Mpanamana reservoir) are biased by the fact that the Eastern boundary of the catchments extends just beyond the Eastern boundary of the high and medium resolution IDEM tiles, i.e. IDEM04 and IDEM10, respectively.

Excluding these two catchments from the analysis of the variation of catchment area, provides evidence for overall consistent estimates. In many cases the coefficient of variation (CV) is less than 1 %. In the worst case (i.e. Rabelais reservoir) the CV reaches a value of 4 %. Analysis of the individual results did not provide any clear evidence for systematic deviations due to the data sets used. However, analysis of the minimum and maximum estimates of catchment size showed that ~ 50 % of the maximum values originated from the use of

the IDEM30 data set and another 30 % from the IDEM10 data set. At the same time, 50 % of the lowest estimates were attributable to the SRTM1 data set. If we assume that the mean catchment area calculated is a good estimate of the true catchment area, then this indicates a tendency of the low and medium IDEM products to overestimate and the SRTM1 product to underestimate catchment area in this rather flat terrain.

Taking into account the number of observations ($N = 5$) the coefficient of variation transforms into a rather small relative uncertainty (Taylor, 1997) of the catchment area estimation between 1 and 5 % on a 95 % confidence level. This indicates a rather high precision of the catchment area estimates and

conforms to the findings of Oksanen and Sarjakoski, 2005. They investigated error propagation in digital elevation models of small catchments ($<5 \text{ km}^2$) derived from high resolution topographic maps and determined the error of catchment size estimations to be 10 % at a maximum on the 95 % confidence level. Unfortunately, no high resolution DTMs are available for extensive areas of the KNP to test the accuracy of the catchment area estimates.

The comparison of the detailed maps presenting the results of the catchment delineation for Jones-se (West) and Silolweni (East) reservoirs based on all discussed DSMs (Figure 9) and reproduced at a scale of $\sim 1:120.000$, provide visual evidence for the new quality of the digital representation of the Earth implemented by the IDEM products. Scrutinizing the IDEM04 map, it becomes clear that the short length roughness elements on the surface, exhibiting clear differences between Jones-se and Silolweni catchment, indeed represent canopy cover structures due to single trees and groups of trees. In a more generalized way, these structures are still discernible in the IDEM10 map, but are basically smoothed out in the IDEM30. This smoothing actually might be of advantage for the routing of discharge. Although it might be difficult to retrace in the medium scale printed maps, there is evidence that the drainage pattern in the higher resolution IDEM maps is quite often laterally shifted due to high and dense riparian vegetation following the thalwegs. This phenomenon is clearly more

common in the flatter Silolweni catchment as compared to the steeper Jones-se catchment (Table 11). Obviously, the rather flat terrain in Silolweni catchment is as well the explanation for the poor performance of the ASTER GDEM2 in the catchment delineation exercise. For the steeper Jones-se catchment the DSM derived from optical images provides a result comparable in catchment form and size (Figure 9).

Finally, the comparison of the medium and low resolution SRTM and IDEM products clearly provide evidence for the engineering progress in the field of satellite-based SAR technology. The IDEM products are obviously largely free of speckle artefacts. This clearly provides new opportunities to characterize the canopy cover of the Earth and geomorphological features in arid areas devoid of vegetation.

3.3 Catchment relief

The high precision and accuracy of the IDEM data sets resulting in comparable catchment delineations and catchment area estimates (Figure 9, Table 10) provides the opportunity to further investigate the variation of catchment property estimates due to changes in the geometric resolution of the fundamental DSM. Generally, it can be anticipated, that estimates of local relief, terrain roughness as well as local and mean slope are reduced with increasing pixel size (Hengl and Evans, 2009).

Name	ID	Mean [km^2]	STD [km^2]	CV [%]
Sable	1	27,688	0,894	3,2
Nhlanganini	2	27,501	0,167	0,6
Ngotso_B	3	16,930	0,068	0,4
Hartbeesfontein	4	4,270	0,131	3,1
Rabelais	5	6,429	0,257	4,0
Marhaya	6	27,473	0,135	0,5
Lugmag	7	47,405	0,114	0,2
Mazithi	8	19,909	0,097	0,5
Ntswiri	9	5,533	0,030	0,5
Jones-se	10	6,205	0,051	0,8
Silolweni	11	13,193	0,353	2,7
N'wanetsana	12	3,248	0,026	0,8
Mlondozi	13	104,191	0,384	0,4
Mestel	14	14,462	0,156	1,1
Mtshawu	15	20,338	0,045	0,2
Shitlhhave	16	2,019	0,033	1,6
Mpondo	17	17,996	0,088	0,5
Newu	18	20,752	0,273	1,3
Stolsnek	19	25,570	0,073	0,3
Nhlanganzwani*	20*	15,952	0,539	3,4
Mpanamana*	21*	9,853	0,242	2,5

Table 10. Statistical analysis of the catchment size [km^2] variation derived from the IDEM and SRTM products ($N = 5$) using Arc Hydro Tools. * denotes catchment areas were the Eastern catchment boundary is affected by the Eastern boundary of the IDEM04 and IDEM10 tiles.

ID	IDEML04	IDEML05	IDEML06
1	3.7 \pm 2.2	2.1 \pm 1.0	1.8 \pm 0.7
2	4.9 \pm 2.7	3.6 \pm 1.7	2.8 \pm 1.2
3	3.1 \pm 1.7	2.0 \pm 0.9	1.6 \pm 0.6
4	4.7 \pm 3.1	2.9 \pm 1.7	2.4 \pm 1.1
5	5.4 \pm 2.7	4.0 \pm 1.3	3.3 \pm 1.1
6	3.6 \pm 2.1	2.0 \pm 1.1	1.8 \pm 0.8
7	4.4 \pm 2.3	3.3 \pm 1.3	2.8 \pm 1.1
8	2.5 \pm 1.8	1.2 \pm 0.7	1.1 \pm 0.4
9	5.6 \pm 2.5	4.5 \pm 1.6	3.8 \pm 1.3
10	6.1 \pm 3.0	4.8 \pm 1.6	4.0 \pm 1.3
11	4.6 \pm 2.6	2.4 \pm 1.2	1.9 \pm 1.0
12	5.6 \pm 2.8	4.4 \pm 1.4	3.6 \pm 1.2
13	4.1 \pm 6.8	3.2 \pm 6.5	2.9 \pm 5.6
14	9.1 \pm 4.9	7.2 \pm 3.0	6.2 \pm 2.7
15	8.3 \pm 5.4	6.8 \pm 4.2	5.8 \pm 3.2
16	6.1 \pm 3.8	5.2 \pm 2.2	4.3 \pm 1.6
17	6.0 \pm 2.7	5.0 \pm 1.7	4.2 \pm 1.4
18	12.5 \pm 8.1	11.1 \pm 7.0	9.0 \pm 5.2
19	12.1 \pm 9.0	10.5 \pm 7.7	8.5 \pm 5.5
20*	4.7 \pm 5.7	3.8 \pm 5.3	3.9 \pm 4.7
21*	6.2 \pm 5.6	5.2 \pm 5.0	5.3 \pm 4.7

Table 11. Statistical analysis of the mean slope \pm STD [%] estimates based on the three IDEM products.

* denotes catchment areas were the Eastern catchment boundary is affected by the Eastern boundary of the IDEM04 and IDEM10 tiles.

Table 11 compiles the mean slope measures, reported in percent rise, derived from the three IDEM data sets for 21 catchments located in the southern part of the KNP. Often, the mean slope derived from the low resolution IDEM30 is about 50 % of the value derived from the high resolution IDEM04 data set. However, due to the fact that the open canopy induces in some locations, i.e. at the edge of trees and group of trees, quite steep 'slopes', it remains unclear, to which extend catchment wide steeper mean slopes derived from the high resolution IDEM04 are representative of the bare ground gradient. Further work is needed to elucidate this question in order to fully exploit the potential of the IDEM products to provide consistent, high resolution catchment properties applicable to geomorphological and hydrological studies in the vast parts of the World were high resolution DTMs from other sources are missing.

4. CONCLUSIONS

The local scale validation of TanDEM-X derived IDEM products with a geometric resolution from 0.4 to 3 arc sec (IDEM04, IDEM10, and IDEM30) using moderate terrain RTK-GNSS based ground survey points with an absolute accuracy of < 0.1 m from a pristine Lowveld Savanna environment provides evidence for the high accuracy of this new and truly global digital elevation model. Including selected, global, open access precursor DEMs, i.e. SRTM1, SRTM90 and ASTER-GDEM2 in the analysis highlights the engineering progress in the field of satellite-based surveying of the Earth.

However, and quite surprisingly, the high precision and accuracy of the IDEM data sets has only little impact when it comes to the delineation of watersheds and the calculation of surface water catchment area. Using 21 catchments of reservoirs within the Kruger National Park ranging in size from a few km² to about 100 km² resulted in differences of often only 1 % when comparing the results derived from the IDEM and the SRTM data sets.

ACKNOWLEDGEMENTS

The IDEM data was provided by the German Aerospace Center (Deutsches Zentrum für Luft- und Raumfahrt (DLR)) under the grant IDEM_Other0118, Kruger National Park Erosion Research DEM (KNPErosIDEM). ASTER GDEM2 is a product of METI and NASA. The SRTM1 data was released by the USGS in September 2014 and the SRTM90 data used here is courtesy of CGIAR-CSI. Field work was conducted in the framework of the KNP Erosion Research Project funded by the German Research Foundation (Deutsche Forschungsgemeinschaft, DFG, grant: BA 1377/12-1). Ample support by SANParks Scientific Services in Skukuza, South Africa, is sincerely acknowledged.

REFERENCES

ASTER GDEM Validation Team, 2011. ASTER Global Digital Elevation Model Version 2 – Summary of Validation Results. http://www.jspacesystems.or.jp/ersdac/GDEM/ver2Validation/Summary_GDEM2_validation_report_final.pdf (25 Mar 2015).

Baade, J., and C. Schmullius, 2014. Uncertainties of a TanDEM-X derived Digital Surface Model. A Case Study from the Roda Catchment, Germany. *Proceedings IGARSS*, 2014: 4327-4330.

Bräutigam, B., M. Bachmann, D. Schulze, D. Borla Tridon, P. Rizzoli, M. Martone, C. Gonzales, M. Zink, and G. Krieger, 2014. TanDEM-X global DEM Quality status and aquisition completion. *Proceedings IGARSS*, 2014, pp. 3390-3393.

Chandler, G., and C. Merry, 2010. The South African Geoid 2010: SAGEOID10. *PositionIT*, 22 (June 2010), pp. 29-33.

Carruthers J., 1995. *The Kruger National Park. A social and political history*. Univ. of Natal Press, Pietermaritzburg, South Africa.

Esri Water Resources Team, 2014. Arc Hydro Overview Document #1. Environmental Systems Research Institute, Inc. (Esri), Redlands, CA, USA.

Farr, T.G., P.A. Rosen, E. Caro, R. Crippen, R. Duren, S. Hensley, M. Kobrick, M. Paller, E. Rodriguez, L. Roth, D. Seal, S. Shaffer, J. Shimada, J. Umland, M. Werner, M. Oskin, D. Burbank and D. Alsdorf, 2007. The Shuttle Radar Topography Mission. *Reviews of Geophysics* 45(2), RG2004, pp. 1-33.

Hengl, T. and I.S. Evans, 2009. Mathematical and digital models of the land surface. In: Hengl, T. and H.I. Reuter, Eds., *Geomorphometry. Concepts, Software, Applications*. Elsevier, Amsterdam, NL, pp. 31-63.

Jarvis A., H.I. Reuter, A. Nelson, and E. Guevara, 2008. *Hole-filled seamless SRTM data V4*, International Centre for Tropical Agriculture (CIAT), available from <http://srtm.csi.cgiar.org>.

Krieger, G., M. Zink, M. Bachmann, B. Bräutigam, D. Schulze, M. Martone, P. Rizzoli, U. Steinbrecher, J.W. Antony, F. De Zan, I. Hajnsek, K. Papathanassiou, F. Kugler, M.R. Cassola, M. Younis, S. Baumgartner, P. Lopez-Dekker, P. Prats, and A. Moreira, 2013. TanDEM-X: A radar interferometer with two formation-flying satellites. *Acta Astronautica* 89(2), pp. 83-98.

Oksanen, J. and T. Sarjakoski, 2005. Error propagation of DEM-based surface derivatives. *Computers & Geosciences* 31, pp. 1015–1027.

Rodriguez, E., C.S. Morris, and J.E. Belz, 2006. A global assessment of the SRTM performance. *Photogrammetric Engineering & Remote Sensing*, 72(3), pp. 249-260.

Venter, F.J., R.J. Scholes and H.C. Eckhardt, 2003. The abiotic template and its associated vegetation pattern. In: Du Toit, J.T., K.H. Rogers and H.C. Biggs, Eds., *The Kruger Experience. Ecology and Management of Savanna Heterogeneity*. Island Press, Washington, USA, pp. 83-129.

Wessel, B., T. Fritz, T. Busche, B. Bräutigam, G. Krieger, B. Schättler, and M. Zink, 2013. TanDEM-X Ground Segment DEM Products Specification Document. Report TD-GS-PS-0021. Issue 2.0. Deutsches Zentrum für Luft- und Raumfahrt, Oberpfaffenhofen, Germany.

Wessel, B., A. Gruber, M. Huber, M. Breunig, S. Wagenbrenner, A. Wendleder, and A. Roth, 2014. Validation of the absolute height accuracy of TanDEM-X DEM for moderate terrain. *Proceedings IGARSS*, 2014, pp. 3394-3397.

Zink, M., and A. Moreira, 2014. TanDEM-X Mission status: The new topography of the Earth takes shape. *Proceedings IGARSS*, 2014, pp. 3386-3389.